SAND2019-4932C
Proceedings of the 2019 Hypervelocity Impact Symposium
HVIS2019
April 14-19, 2019, Destin, FL, USA
HVIS2019-072

Numerical and Experimental Evaluations of a Glass-Epoxy Composite Material Under High Velocity Oblique Impacts

Christopher T. Key[a,*], C. Scott Alexander[b]

[a]*Applied Physical Sciences Corp., 475 Bridge Street Suite 100, Groton CT, 06340, USA*
[b]*Sandia National Laboratories, PO Box 5800, Albuquerque NM, 87185, USA*

Abstract

Composite materials are used as alternatives to conventional metallics in a multitude of applications including military ground vehicles, aircraft, space launch and re-entry vehicles and even personnel protection where weight savings are critical. In application, these materials are susceptible to high velocity impacts from various threats and it is essential that the response of these materials, under relevant conditions, be understood in order to provide optimized effective designs. This work details an on-going effort to validate the anisotropic multiple constituent model (MCM) within the CTH hydrocode. Within the CTH framework, the anisotropic MCM model is coupled with an equation of state (EOS) and provides continuum averaged stress and strain fields for each constituents (fiber and resin) of a composite microstructure from which progressive damage evaluations can be performed. In this paper we focus on recent validation efforts where woven S2/SC15 (glass/epoxy) composite panels were impacted with steel spheres at various impact velocities and angles of obliquity. The experimental testing was performed at the Shock Thermodynamics Applied Research (STAR) Facility at Sandia National Laboratories to provide data for further validation of the MCM model under oblique impact conditions. Oblique impacts result in stress fields which exercise the anisotropy of the strength model and EOS coupling of the MCM model more robustly. Results are presented for both the CTH MCM model predictions and the experimental testing results. The primary comparison metrics evaluated are the predicted and observed damage extent, overall damage pattern, and residual velocity of the sphere.

Keywords: Composite Material, Hydrocode, Oblique Impact, Damage, Residual Velocity

1. Introduction

Composite materials are widely used in both the defense and commercial sectors for various applications. Many of these applications present the possibility of the composite material being subjected to high-velocity impacts, where the strain rates can be on the order of 10^6 s^{-1} or more and the pressures are often in the tens of *GPa*. The work presented in this paper expands upon previous work for the same materials where the impacts were normal to the composite material [1] by considering the non-ideal condition of oblique impacts that is more likely than not to occur in regular use. The ability to simulate and capture the composite material response under these oblique conditions is essential. Similar to the normal impact work, this effort focuses on both the go/no-go metric for impact penetration and the ability of the numerical simulations to predict the extent of the damage caused by these impacts. The metric of post-impact damage is critical as it relates to stiffness and strength degradations that may reduce the structural integrity and the penetration resistance for subsequent impacts.

In order to capture the appropriate physics responses for these high-velocity and large strain impact problems, the shock physics hydrocode CTH [2] was used to model the impact event and subsequent response of the composite material. The challenge of utilizing a hydrocode for these simulations is that for traditional isotropic materials such as steel or aluminum, the material response is split into an uncoupled hydrostatic (pressure) component and a deviatoric (strength) component. However, for an

* Corresponding author. Tel.: +1-307-760-8799; fax: +1-860-448-3075.
E-mail address: ckey@aphysci.com

anisotropic material such as the fiber-reinforced composite considered herein, the deviatoric and hydrostatic responses are coupled. Therefore, an anisotropic model must be used which couples the equation of state (hydrostatic response) and the strength response. The multi-constituent composite model (MCM) [3] within CTH provides such a model where the strength and EOS responses are coupled. The MCM model also provides an advanced damage model which allows for the prediction and degradation of the composite material response according to the mode of damage achieved.

This paper details both the oblique impact experimental testing and the associated numerical modeling efforts which evaluate the oblique impact response and damage evolution of an S-2 glass / SC15 epoxy woven fabric composite material. The experimental configuration consisted of 6.35 mm (¼") diameter steel spheres impacting composite panels at obliquity angles of 22.5°, 45°, 56.2° and 67.5° at velocities up to 1000 m/s in order to generate a range of damage to the targets including both penetrating and non-penetrating events. High speed cameras were utilized to capture the impact event and also measure the residual velocity for those conditions where the projectile did not embed in the composite target. After testing, backlit photographic images were used to evaluate the extent of damage imparted on the panels for comparison with the numeric predictions.

In the following sections, we briefly outline the MCM composite material constitutive and damage model along with the equation of state coupling approach. Next, a description of the experimental setup is detailed. Finally, comparisons are made between the analytical simulations which utilized the MCM model to predict both the residual velocity and the associated damage extent of each tested impact condition.

2. MCM Model Overview

The multiple constituent model (MCM) provides the micro-scale constituent (i.e. fiber and matrix) level responses of a composite microstructure without the need to model the micromechanical details explicitly. This means that one can model macroscopic objects and still capture the constituent level details without explicitly resolving the microscopic details.

In order to accomplish this, the MCM model leverages micromechanics simulations run *a priori* to extract volume averaged constituent stress and strain fields. Specifically, the MCM model assumes that at each continuum point within a macro-scale structure, there exists a representative volume element (RVE) or repeating microstructure. For the case of a woven fabric composite material considered herein, Figure 1 illustrates the RVE, where the warp bundles are shown in white, the weft bundles are shown in orange and the interstitial resin pockets have been removed for clarity.

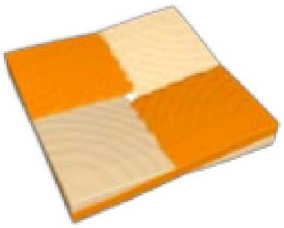

Figure 1. Plain Weave Composite Representative Volume Element (RVE).

Equation (1) is the fundamental relationship for the MCM model from which the volume averaged constituent strain fields are extracted from the individual constituent volume fractions (ϕ), composite strain fields (ε) and a concentration tensor (A) which is a function of the composite and constituent stiffness matrices.

$$\{\varepsilon_{fiber}\} = \left(\phi_{fiber}[I] - \phi_{resin}[A]\right)^{-1}(\{\varepsilon\}) \tag{1}$$

The volume averaged constituent stress fields can similarly be determined using their respective linear elastic constitutive relationship.

It is important to note here that Equation (1) decomposes the composite strain field for a two constituent system (i.e. fiber and

resin). Therefore, for the woven fabric microstructure where there are assumed to be three constituents (warp bundle, weft bundle and pure resin pockets), the decomposition relationships presented in Equation (1) must be applied successively to obtain the stress and strain fields for each of the 3 constituents in the microstructure. A Schematic of this successive decomposition approach is shown in Figure 2.

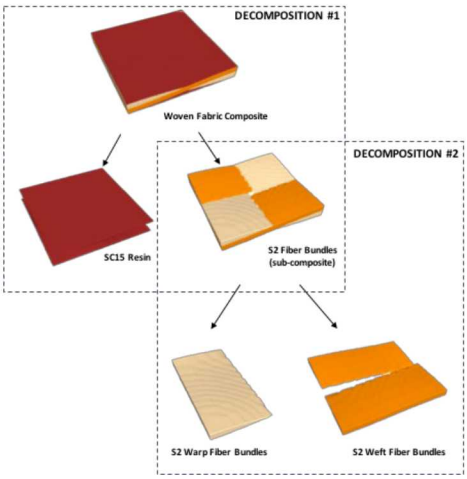

Figure 2. Plain Weave (3-Constituent) Decomposition.

The reader is referenced to Hill [4], Garnich and Hansen [5] and Key [6] for a detailed derivation and description of the MCM modeling approach.

2.1 MCM Progressive Damage Model

The damage and failure criterion within the MCM model treats each of the fiber bundles of the woven fabric microstructure as individual unidirectional composites such that the transversely isotropic failure criterion developed by Hashin [7] can be applied to the bundles individually. The basic failure criteria for the fiber and resin dominated directions within the fiber bundles are given in Equations (2-3) where $D_{\#}$ represents the strength coefficients and $I_{\#}$ are the transversely isotropic strain invariants which were chosen based on previous work [8,9].

$$\pm D_1^f (I_1)^2 + D_4^f I_4 <= 1 \tag{2}$$

$$\pm D_2^m (I_2)^2 + D_3^m I_3 + D_4^m I_4 <= 1 \tag{3}$$

When damage is predicted to occur according to these criteria, the constituent and composite stiffnesses are degraded consistently with the finite element based micromechanics models run *a priori*. The interested reader is referred to [8, 10] for a more detailed development of these criterion.

2.2 Equation of State Coupling

The MCM model also contains an anisotropic coupling algorithm which accounts for the coupling between the pressure (EOS) and deviatoric stress components which is necessary in a conventional hydrocode formulation. For this work, a coupling approach developed and detailed by Lukyanov [11,12] was used. Equation 4 shows the anisotropic stress decomposition relationship of Lukyanov used for the MCM model, where P_{EOS} is the pressure directly from the equation of state, $\tilde{S}_{ij}$ is the generalized deviatoric stress tensor and α_{ij} and β_{ij} are the coupling tensors which are a function of the material stiffness and compliance, respectively. It is noted that these coupling tensors are formulated such that when combined with the deviatoric stress, the deviatoric strains are zero.

$$\sigma_{ij} = -\left(P^{EOS} + \frac{\beta_{ij} S_{ij}}{\alpha_{ij}\beta_{ij}}\right)\alpha_{ij} + \tilde{S}_{ij} \quad (4)$$

3. Materials and Experimental Setup

The target materials for all testing performed in this study were comprised of S-2 glass / SC15 epoxy composite. Samples tested were all 6.35 mm (¼") thick and were manufactured with a [0/90] layup. All material stiffness, strength and equation of state parameters used for this material are detailed in [1]. The projectiles were 6.35 mm (¼") diameter spheres composed of soft carbon steel (type 1018).

The high velocity oblique impact experiments for this work were performed at Sandia National Laboratories using single and two stage light gas guns. This work follows similar oblique impact testing which has been performed by other researchers on various composite material systems in the past [13-15]. The composite panels were mounted in a test fixture for each test as shown in Figure 3. The test panel was mounted using light pressure applied with set screws around the perimeter to approximate an unconfined panel (no edges of the panel were rigidly confined). Upon impact, the panel is allowed to move with very little force. Panels were mounted such that impact was intended to be in the center of the panel. The spheres were launched at velocities from 300 to 1000 m/s with obliquity angles of 22.5°, 45°, 56.2 and 67.5° as defined in Figure 4.

Figure 3. Ballistic testing experimental test fixture. Setup shown is for impact obliquity of 22.5 degrees.

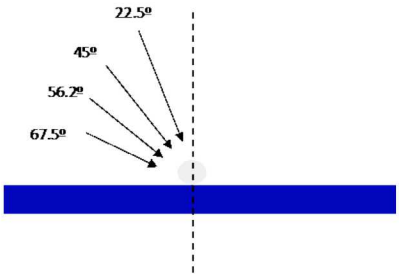

Figure 4. Obliquity Angles for Experimental Testing.

For each test, a single sphere was mounted in a two-part sabot. The sabot is launched at the desired velocity and then separated aerodynamically by introducing a small atmosphere in the experimental range and stripped by steel barriers. The sphere passes through a Magnetic Velocity Induction System (MAVIS), an external magnetic field and a pair of pickup coils, prior to impact to determine the impact velocity.

The impact event is monitored with high speed video. Three Phantom V2511 cameras running at 200,000 frames per second were used. Two cameras were set up with a view orthogonal to the flight line of the projectile. The third camera observed the rear surface of the target. The combination of cameras resulted in an excellent field of view on both sides of the composite plate and provided a rear surface view showing time resolved extent of damage.

4. Results

4.1 Residual Velocity

The first metric used to evaluate the MCM model predictions against the experimental testing results was the residual velocity of the penetrator. The residual velocity predicted by the MCM model and measured during the experimental testing are shown below in Table 1, where the table is color coded using green for conditions where the projectile was defeated by the composite target plate and orange for conditions where the projectile defeated the target plate. The simulations were conducted *a priori* and as a result there are minor differences between the simulated and tested impact velocities. Untested velocities where defeat could not be inferred are left uncolored.

Table 1. Simulation results for oblique impacts.

Impact Velocity (m/s)	22.5°	
	Residual Velocity (m/s)	
	CTH – MCM Simulation	Experimental
300	DNP	-
345	-	DNP
400	DNP	DNP
455	-	61
500	130	-
517	-	220
600	260	-
700	370	-
800	475	-
900	575	-

Impact Velocity (m/s)	45°	
	Residual Velocity (m/s)	
	CTH – MCM Simulation	Experimental
300	DNP	-
400	DNP	-
417	-	DNP
500	20	-
530	-	DNP
600	60	-
609	-	234
700	230	-
705	-	428
800	350	-
1000	525	-

Impact Velocity (m/s)	56.2°	
	Residual Velocity (m/s)	
	CTH – MCM Simulation	Experimental
400	DNP	-
419	-	DNP
447	-	DNP
500	DNP	-
600	DNP	-
647	-	238
700	DNP	
777	-	465
800	50	-
900	250	-
1000	350	-

Impact Velocity (m/s)	67.5°	
	Residual Velocity (m/s)	
	CTH – MCM Simulation	Experimental
500	DNP	-
593	-	DNP
600	DNP	-
700	DNP	-
717	-	DNP
777	-	279
800	DNP	-
855	-	438
900	DNP	-
1000	DNP	-

The results summarized in Table 1 show that the MCM model predictions are in good agreement with the experimental results for the 22.5° impact condition, where both penetrate/no-penetrate conditions are between 400 and 500 m/s. For this obliquity, the residual velocity for the MCM model was calculated to be 130 m/s at an impact velocity of 500 m/s while the experimental residual velocity was measured to be 220 m/s at an impact velocity of 517 m/s. For the 45° configuration, the MCM model predicts penetration at approximately 600 m/s while the experimental results indicate the penetrate/no-penetrate impact condition to be between 530 and 609 m/s. A calculation at 500 m/s impact velocity indicated penetration with a residual velocity of 20 m/s. However, under these conditions, penetration occurred slowly over a much longer time scale than other conditions making it unclear if this result clearly indicates a prediction of penetration. At obliquity angles greater than 45° an increasing angle results in a divergence of the MCM model predictions from the experimental results. For the 56.2° configuration the simulations predicted a penetrate/no-penetrate impact condition between 700 – 800 m/s, while the experimental data resulted in penetration occurring between 447 and 647 m/s. Finally, for the 67.5° configuration the MCM model simulation were run up to an impact velocity of 1000 m/s under which each simulation predicted that the projectile would not penetrate the panel and would instead deflect. However, under the experimental testing efforts a penetration event for this configuration was observed to occur between 717 and 777 m/s with a residual velocity of 279 m/s for the 777 m/s impact condition.

4.2 Damage Pattern and Extent

The second metric used to compare the MCM model predictions and the experimental testing results was a qualitative comparison of the impact induced damage pattern and extent on the panels. The extent of damage from the MCM model was measured from plots of the predicted damage states, while the extent of damage in the experiments was measured from backlit photographs of the post impact specimens. Damage is quantified by measuring the horizontal extent of damage, referred to as width, and the vertical extent, measured above and below the impact point. Additionally, the bias ratio, or the ratio of the vertical extent of damage above to below the impact point is used.

Comparison of the predicted and measured damage patterns and extent for the 22.5° specimens at ~500 m/s are shown below in Figure 5. This image shows that the extent of damage is similar between the simulations and experiment. Specifically, the MCM model predicted a damage width of 6.35 cm (2.5”) while the measured width from the experiment was 7.87 cm (3.1”). Similarly, the predicted damage above and below the impact point for the simulations was 3.0 cm (1.18”) and 4.09 cm (1.61”), respectively; while the experimental testing resulted in damage extents of 3.63 cm (1.43”) above the impact point and 1.74” below the impact point. These measured damage extents correspond to bias ratio defined as the above impact extent to the below impact extent of 0.73 for the simulations and 0.82 for the experiment which are considered to be in good agreement. One point of note is that the damage pattern predicted by the MCM model is more of a “+” type pattern while the experimental backlit images reveal more of an oval pattern. As detailed in the normal impact results [1], this difference is likely due to the lack of an interstitial failure mode in the current MCM failure criteria and the inability to capture delamination planes in the Eulerian framework of CTH.

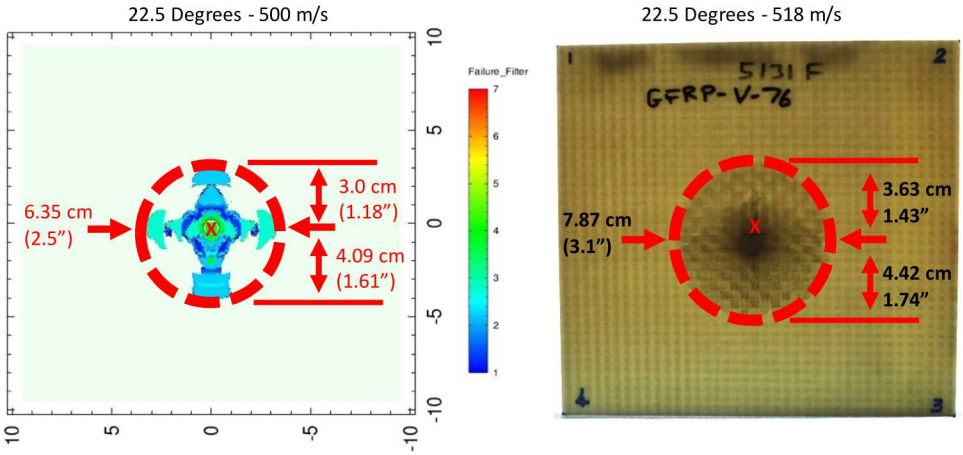

Figure 5. Predicted and experimentally observed damage pattern and extent for 22.5° obliquity at ~500 m/s impact.

Similar to the 22.5° specimens, the 45° specimen shown in Figure 6 shows good agreement in the extent of damage and bias ratio between the predictions and the experiments. Specifically, the MCM model predicted a damage width of 5.89 cm (2.32”) with an extent of 3.2 cm (1.26”) above the impact point and 5.13 cm (2.08”) below the impact point, resulting in a bias ratio of 0.6. The corresponding experimental test resulted in a damage width of 7.47 cm (2.94”) with a damage extent of 2.87 cm (1.13”) above the impact point and 4.98 cm (1.96”) below the impact point, or a bias ratio of 0.58. Also similar to the 22.5° obliquity impact condition, the model predictions show more of a discrete cross or “t” pattern as compared to the oval pattern in the experimental test which is again likely due to the lack of interstitial failure modes in the model.

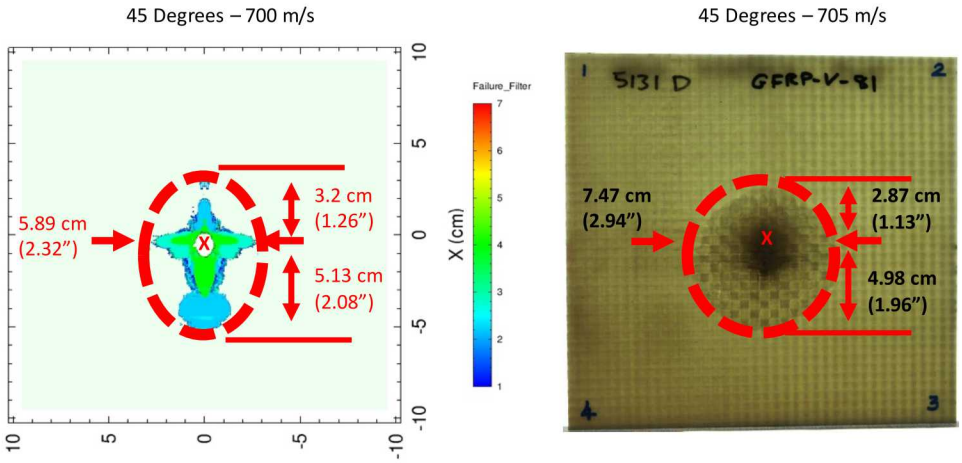

Figure 6. Predicted and experimentally observed damage patterns and extents for 45° obliquity at ~700 m/s impact.

For the 67.5° impact condition shown in Figure 7, the model predicted a damage width of 6.71 cm (2.64”) with an extent of 1.27 cm (0.5”) above the impact point and 6.0 cm (2.36”) below the impact point (bias ratio = 0.21), while the experimental test resulted in a damage width of 8.05 cm (3.17”) with a 2.87 cm (1.13”) extent above the point of impact and 6.35 cm (2.5”) below the point of impact (bias ratio = 0.45). Although the bias ratio is larger for the experimental testing, this is likely due to the fact that the simulations did not predict complete penetration of the panel at 800 m/s which would lead to a lesser damage extent on the exit face. Again, the model predictions result in a cross or “t” pattern which is different than the experimental results. However, it is noted that the damage pattern predicted by the model does correspond fairly well with the black regions of the test specimen photo corresponding to highly damaged material.

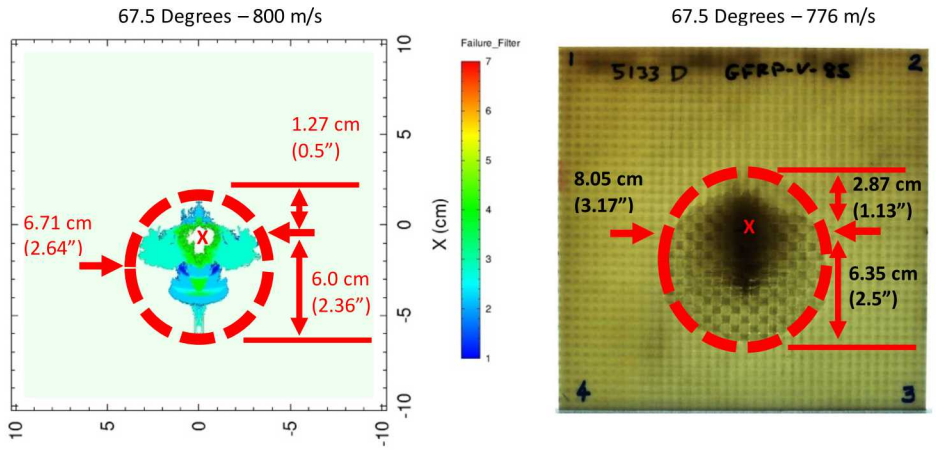

Figure 7. Predicted and experimentally observed damage patterns and extent for 67.5° obliquity at ~800 m/s impact.

Damage results are not shown herein for 56.2° obliquity for brevity. However, results for this configuration followed the trends indicated previously. The extent of damage was slightly underpredicted in the model falling intermediate to the 45° and 67.5° cases as expected with more of a cross type damage pattern as observed in 45° and 67.5°.

5. Conclusions

Overall, the results shown in this paper demonstrate that the MCM model provides good correlation in residual velocity for obliquity angles up to 45°. The model also shows good agreement in damage extent with the experimental results throughout all angles of obliquity studied, with a limited set of comparisons shown herein. The results show that the MCM model predicted penetrate/no-penetrate level begins to diverge from the experimental results as the obliquity angle increases with divergence becoming apparent for angles over 45°. This divergence is believed to be a function of both the longitudinal equation of state parameters and the fiber dominated strength coefficients of the model which are exercised under the increased obliquity angles. Future work will utilize this new data to improve the model and model parameters under these increased obliquity conditions.

Acknowledgements

The views expressed in the article do not necessarily represent the views of the U.S. Department of Energy or the United States Government.

Sandia National Laboratories is a multimission laboratory managed and operated by National Technology & Engineering Solutions of Sandia, LLC, a wholly owned subsidiary of Honeywell International Inc., for the U.S. Department of Energy's National Nuclear Security Administration under contract DE-NA0003525.

References

[1] Key, C.T. Alexander, C.S., 2018. Experimental Testing and Numerical Modeling of Ballistic Impact on S-2 Glass/SC15 Composites, Journal of Dynamic Behavior of Materials, 4(3): 373-386.
[2] McGlaun, J.M., Thompson, S.L., Kmetyk, L.N. and M. G. Elrick, 1990. A brief description of the three- dimensional shock wave physics code CTH, Sandia National Laboratories report SAND89-0607.
[3] Schumacher, S.C., Key C.T. 2012. CTH Reference Manual: Composite Capabilities, Sandia National Laboratories Report SAND2012-7714.
[4] Hill, R. 1964. Theory of Mechanical Properties of Fibre-Strengthened Materials: I. Elastic Behavior, Journal of Mechanics and Physics of Solids 12, 199-212.
[5] Garnich, M.R., Hansen, A.C. 1997. A multicontinuum theory for thermal-elastic finite element analysis of composite materials, Journal of Composite Materials 31(1): 71-86.
[6] Key, C.T., Six R.W., Hansen, A.C., 2003. A three-constituent multicontinuum theory for woven fabric composite materials, Composites Science and Technology 63(13): 1857-1864.
[7] Hashin, Z. 1980. Failure criteria for unidirectional fiber composites, Journal of Applied Mechanics 47(6): 329-349.
[8] Key, C.T., Schumacher, S.C., Alexander, C.S., 2015. Evaluation of a strain based failure criterion for the multi-constituent composite model under shock loading, DYMAT 2015 Conference on Mechanical and Physical Behaviour of Materials under Dynamic Loading, Lugano, Switzerland, 7-11 September.
[9] Gorfain, J.E., Key C.T., 2013. Damage prediction of rib-stiffened composite structures subjected to ballistic impact, International Journal of Impact Engineering 57: 159-172.
[10] Mayes J.S., Hansen, A.C., 2004. Composite laminate failure analysis using multicontinuum theory, Composites Science and Technology 64(3): 379-394.
[11] Lukyanov, A.A., 2006. Thermodynamically consistent anisotropic plasticity model, Proceedings of IPC2006, 6th International Pipeline Conference.
[12] Lukyanov, A.A., 2008. Constitutive behavior of anisotropic materials under shock loading, International Journal of Plasticity 24: 140-176.
[13] Lamontage, C.G., Manuelpillai, G.N., Taylor, E.A., Tennyson, R.C., 1999. Normal and oblique hypervelocity impacts on carbon fibre/peek composites, International Journal of Impact Engineering, Vol. 23, Issue 1, Part 2, 519-532.
[14] Hazell, P.J., Kister, G., Stennett, C. Bourque, P., Cooper, G., 2008. Normal and oblique penetration of woven CFRP laminates by a high velocity steel sphere, Composites Part A: Applied Science and Manufacturing, 39 (5), 866-874.
[15] Rajagopal, A., Naik, N.K., 2013, Oblique ballistic impact behavior of composites, International Journal of Damage Mechanics, 23 (4), 453-482.